Spin-polarized scanning tunneling microscopy study of Mn/Co/Cu(001) using a bulk Fe ring probe

Chii-Bin Wu, Jiaming Song, and Wolfgang Kuch

Citation: Applied Physics Letters **101**, 012404 (2012); doi: 10.1063/1.4733343
View online: http://dx.doi.org/10.1063/1.4733343
View Table of Contents: http://scitation.aip.org/content/aip/journal/apl/101/1?ver=pdfcov
Published by the AIP Publishing

Spin-polarized scanning tunneling microscopy study of Mn/Co/Cu(001) using a bulk Fe ring probe

Chii-Bin Wu (吳啓彬), Jiaming Song (宋佳明), and Wolfgang Kuch
Institut für Experimentalphysik, Freie Universität Berlin, Arnimallee 14, 14195 Berlin, Germany

(Received 6 March 2012; accepted 20 June 2012; published online 3 July 2012)

A bulk ring probe made of pure iron wire with diameter of 0.125 mm was prepared for spin-polarized scanning tunneling microscopy at room temperature in ultrahigh vacuum. The layerwise antiferromagnetic spin contrast of 2.8 atomic monolayers (ML) Mn/4.5 ML Co/Cu (001) observed with such a probe revealed a spin asymmetry of 14% and a signal-to-noise ratio of 1.8. Areas of reversed spin contrast on the same atomic layer of Mn were observed and attributed to the influence from underlying Co steps and islands. This demonstrates the simplicity of preparation and capability of such bulk Fe ring probes. © *2012 American Institute of Physics*. [http://dx.doi.org/10.1063/1.4733343]

Spin-polarized scanning tunneling microscopy (SP-STM) has been developed for more than twenty years.[1] Its capability of resolving spin structures down to the atomic scale has been utilized in many studies of antiferromagnetic nanostructures on thin film surfaces.[2] Since SP-STM relies on the spin-dependent tunneling effect, the preparation of spin-polarized probes is always a key issue in implementing SP-STM.[1] Over the decades, many different materials and preparation methods have been proposed, e.g., bulk ferromagnetic tips,[3–9] bulk antiferromagnetic tips,[3,5,10–13] ferromangetic thin film coated W tips,[14,15] antiferromagnetic thin film coated W tips,[16,17] local tunneling magnetoresistance mode with CoFeSiB tip[18] and with Fe coated CoFeSiB ring,[19] Fe coated W ring,[20] etc. There are three main issues in choosing the probe for SP-STM. First, there must be spin polarization for the atom that contributes the tunneling current. Second, the influence of the probe on the sample should be as small as possible. Third, it should be possible to control the probe's spin polarization direction in order to identify in which direction the spin component is resolved. Bulk ferromagnetic tips fulfill the first requirement but have the disadvantage of emitting stray field, which might influence the sample's magnetization. Bulk antiferromagnetic tips have no such problem, but their spin polarization direction cannot be controlled easily. That is why ferromagnetic thin film coated W tips are often used instead. However, this requires special treatment of the tip surface before thin film coating, and bears the possibility to loose coated thin film material after *in situ* tip treatment. Therefore, one has to carefully choose the tip for the system under study.

Although thin film coated W tips are often used to implement SP-STM, the axial symmetry of the tip's shape makes it difficult to control the in-plane direction of the tip's spin polarization. To avoid this disadvantage, Fe-coated W rings have been proposed and demonstrated in Ref. 20, where a W ring having a wire diameter of 0.125 mm is first fabricated and then electron bombarded in ultrahigh vacuum, followed by Fe depositon on the probe's surface. Despite its bulky shape, the spatial resolution of such ring probe can reach sub-nanometer, and the stray field seems not to be an issue for the sample studied there. Based on this, here we go a step further and use a bulk ferromagnetic ring probe for SP-STM. There are several advantages in doing so. First, the preparation of bulk Fe ring probes is even much easier than of Fe-coated W rings. This makes the preparation of such probes more reliable. Second, since the scanning probe is of bulk material, one has always the possibility to regain spin polarization after *in situ* tip treatment, e.g., voltage pulse application. Third, the shape anisotropy is stronger than that of the Fe coated W ring, thus one has better control over the probe's magnetization direction. Therefore, the bulk Fe ring probe is a promising candidate for resolving in-plane spin structures with SP-STM.

To prepare such a ring probe, a Fe wire with diameter of 0.125 mm and purity of 99.5% is first magnetized along its axial direction with a permanent magnet and polished with sand paper along the axial direction, too. Wound into ring shape with ring diameter around 1 mm, it is spot-welded onto the tip carrier with the ring plane vertical or horizontal. Since the sample is mounted with its surface plane vertical, this provides spin-sensitivity along two orthogonal axes within the sample surface. A photograph of the ring probe is shown in the inset of Fig. 1(a). After ultrasonic cleaning, it is loaded into ultrahigh vacuum. A sputtering procedure with 2 keV Ar^+ bombardment is necessary to remove the surface oxide and contamination. After this, the ring probe is transferred to the STM and ready for use. Depending on the condition of each probe, another sputter cleaning might be needed before the sample preparation.

To test such a ring probe, an antiferromagnetic sample with a flat surface and ordering temperature above room temperature is preferred, e.g., Mn/Co/Cu(001). When the coverage is less than 10 monolayers (ML), Mn grows in layer-by-layer mode on Co/Cu(001).[21] The Mn shows antiferromagnetic order at room temperature if its thickness is higher than 2.5 ML, while Co with thickness larger than 2 ML on Cu(001) is ferromagnetic at room temperature.[22] The spin structure of Mn in this system has been studied before,[29,30] and a layerwise antiferromagnetic spin structure was observed. The sketch in Fig. 1(a) illustrates such a spin configuration and the possible influence from the surface roughness of the underlying Co layer.

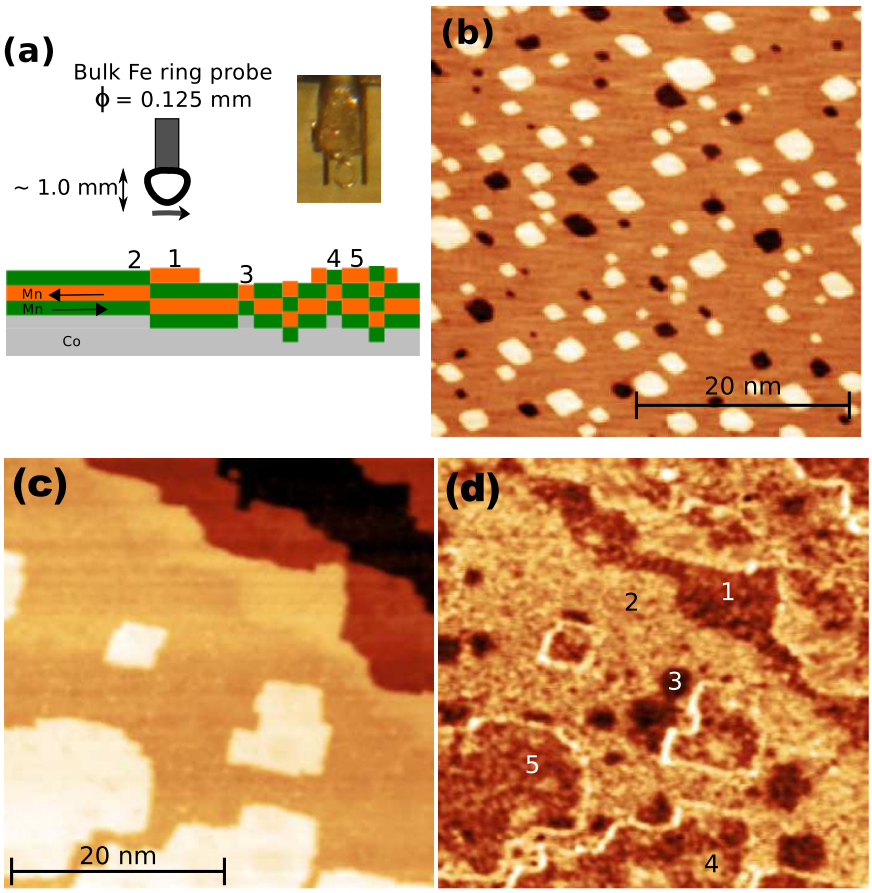

FIG. 1. (a) Schematic drawing of bulk Fe ring probe scanning on Mn/Co/Cu(001), where Mn is assumed to have a layerwise antiferromagnetic spin structure. Numbers 1 to 5 represent different cases of Mn grown on the Co film. The inset shows a photograph of the Fe ring probe. (b) STM topography image of 8.1 ML Co/Cu(001) grown at room temperature. Feedback parameters: gap voltage +0.2 V and tunneling current 1.6 nA. (c) and (d) are STM constant-current-mode images of topography and differential conductance map from the same area of a 2.8 ML Mn/4.5 ML Co/Cu(001) sample at room temperature. Feedback parameters: gap voltage +0.2 V and tunneling current 2.0 nA. The field of view is 50×50 nm^2. The numbers from 1 to 5 in (d) represent different typical places as indicated in (a).

The Cu(001) substrate is cleaned by a sputtering-annealing procedure. The cleanliness of the sample is checked by a four-grid-type Auger electron spectrometer, and the crystalline structure is confirmed by low-energy-electron-diffraction. Cobalt from a rod with purity of 99.95% is evaporated by electron beam bombardment, controlled by a flux monitor. Mn pieces with purity of 99.95% are used to evaporate from a Mo crucible with the same heating method. Both Mn and Co are deposited at room temperature. The thickness of each film is checked by the relative Auger intensities. STM measurements are performed in an Omicron room temperature STM.

To obtain spin signal, the local differential conductance is measured using the lock-in technique. A small modulation of 20 mV is added to the DC gap voltage, and the resultant oscillation amplitude of the tunneling current is detected by the lock-in amplifier. Far from the tunneling regime, the phase of the lock-in amplifier is adjusted such that the output is zero. By this procedure, one can get the differential conductance quantitatively. During constant-current-mode scanning, the topography as well as the local differential conductance at this gap voltage are recorded simultaneously. Since the surface consists of Mn only, we expect the difference in differential conductance to come only from spin signal, except at step edges. This method for obtaining spin signal has been utilized in many studies, see, e.g., Refs. 23, 24, and 17.

In Fig. 1(b), the surface of 8.1 ML Co/Cu(001) grown at room temperature is shown. Co islands of monatomic height can be observed, which have feature sizes of several nanometers. Figs. 1(c) and 1(d) illustrate the SP-STM result on 2.8 ML Mn/4.5 ML Co/Cu(001). The topography image in Fig. 1(c) is obtained in constant current mode with a gap voltage of +0.2 V and feedback current of 2.0 nA. Islands of monatomic height can be observed on the surface. The local differential conductance map of the same area is shown in Fig. 1(d). Clearly, two distinct contrast levels can be observed. For most of the cases, the islands have lower differential conductance than the terrace in between. However, several exceptions are noted. First, although location 1, representing elongated areas near the edge of the terrace, seems to sit on the same terrace as location 2, its contrast level is lower. Second, location 3, representing a small area on one terrace, also has lower contrast than the terrace. Third, location 4, representing a small area on the island, has higher contrast level compared to that of the surrounding island, e.g., location 5.

These reversed contrast phenomena are also observed in other areas of the same sample. Fig. 2 shows more detailed results. The topography image in Fig. 2(a) is obtained with a gap voltage of +0.5 V and feedback current of 2.0 nA, while its corresponding differential conductance map is shown in Fig. 2(b). The interlayer distance is 201 pm, as determined from the histogram in Fig. 2(e). On the flat terraces, some areas with slightly lower height can be distinguished. From the profiles along lines A and C, depicted in Figs. 2(c) and 2(d), respectively, the difference between terrace and these dip areas is around 20 pm. The transition width across a step edge is less than one nanometer. The histogram of the local differential conductance map, shown in Fig. 2(f), reveals two levels of 3.98 nS and 5.30 nS. The edges of the islands shown in Fig. 2(a) are marked with dotted lines and

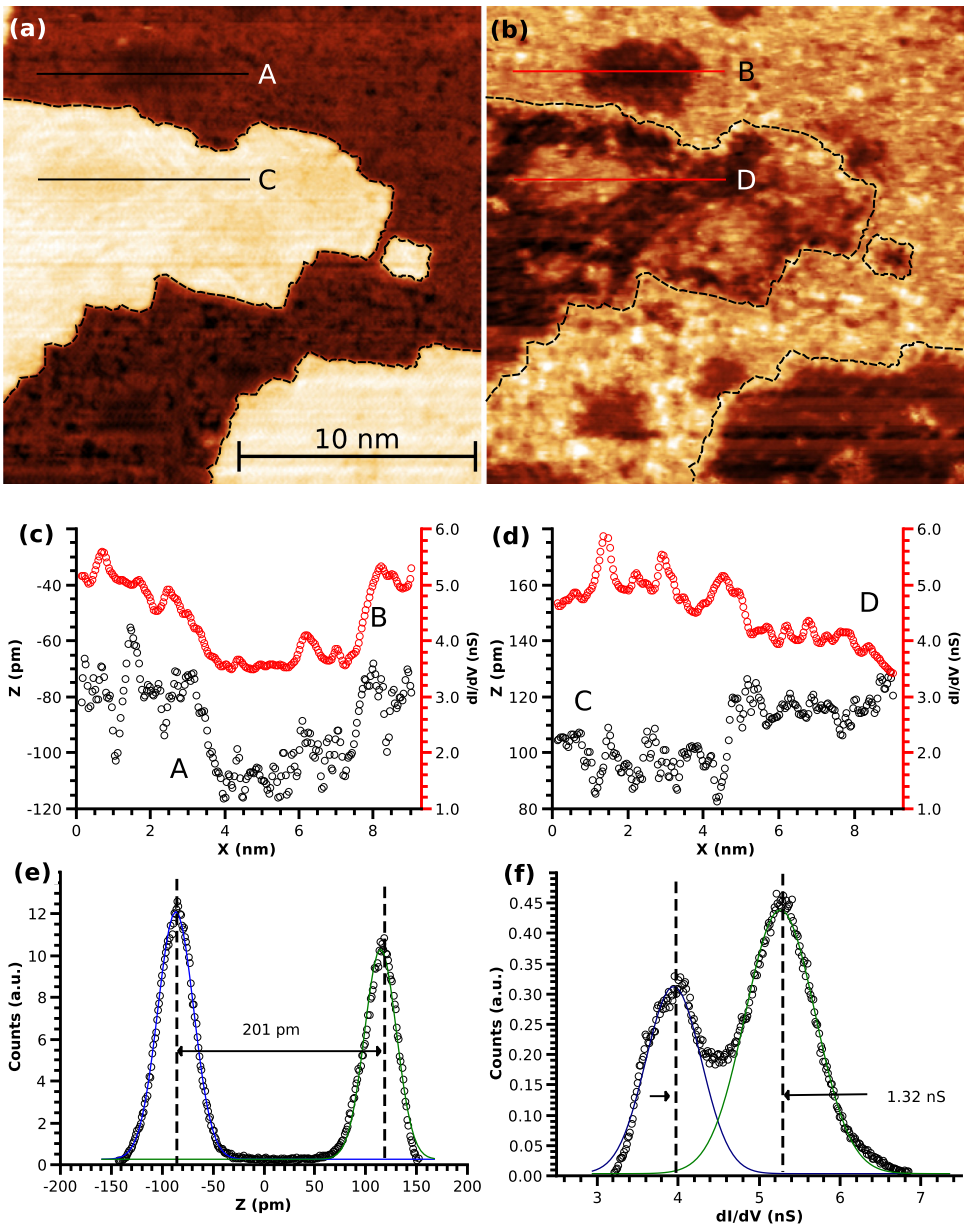

FIG. 2. STM constant current mode images of topography (a) and differential conductance map (b) of the same area of 2.8 ML Mn/4.5 ML Co/Cu(001) at room temperature. Feedback parameters: gap voltage +0.5 V and tunneling current 2.0 nA. The field of view is 20×20 nm^2. The profiles along lines A and B are depicted in (c) while those along C and D are depicted in (d). The histograms of images (a) and (b) are shown in (e) and (f), respectively.

depicted in Fig. 2(b). Overall, the islands have smaller differential conductance than the terrace areas, consistent with the obervation in Fig. 1. Also, areas with reversed contrast on the same island are observed, as well as on the terrace. The line profiles B and D taken at the same location as profiles A and C, respectively, are shown in Figs. 2(c) and 2(d). Line profiles A and B both have lower values in the middle region. However, while line profile C has a lower value in the left, a higher value is observed in the left part of profile D. Most important of all, these changes in topography and differential conductance coincide. The dip regions are always matching the areas with reversed contrast.

To explain the origin of these differences of differential conductance, full spectroscopy measurements are performed on almost the same area, with the gap voltage ramped from +0.5 V to −0.5 V. The feedback parameters in constant current mode are +0.5 V gap voltage and 2.0 nA feedback current. Fig. 3(a) is the topography image, showing almost the same area as Fig. 2. The current map at +0.2 V is shown in Fig. 3(b), where similar layer-wise contrast and areas of reversed contrast can be observed. However, the overall contrast is reversed as compared to Fig. 2(b). The representative I-V curves of the bright and dark areas are shown in Fig. 3(c), where the red (black) curve corresponds to the red (black) area indicated by dashed lines both in Figs. 3(a) and 3(b). The red and black dotted curves are the dI/dV spectra numerically differentiated from the red and black I-V curves, respectively. At a gap voltage of +0.5 V, both curves have current values around 2.0 nA, since this is the feedback condition, but the black curve has a larger slope than the red one. At a gap voltage of +0.2 V, the current value of the black curve is smaller than that of the red one. This explains the contrast inversion between Figs. 2(b) and 3(b).

All of these data can be explained in the model of layerwise spin components for Mn on Co/Cu(001) observed in Refs. 29 and 30, very similar to Mn/Fe(001).[25] According to spin-dependent tunneling theory, the tunneling current depends on the relative orientation of the magnetization of the two spin polarized electrodes, with the current asymmetry proportional to the cosine of their relative angle.[26] Since we use the same Fe ring probe during scanning, if Mn has layerwise spin component (not necessarily collinear), we can

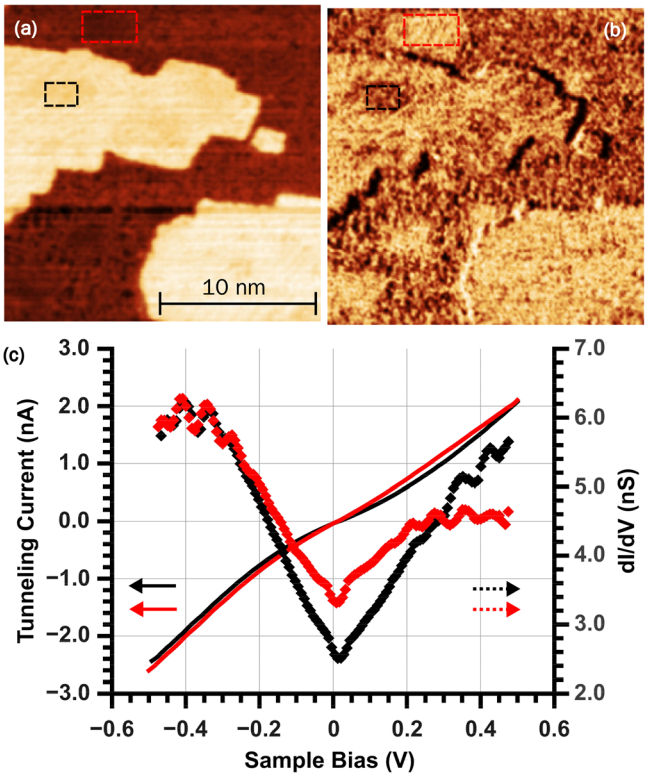

FIG. 3. (a) Topography and (b) current map at +0.2 V obtained in full spectroscopy mode on roughly the same area as Fig. 2(a). The black and red I-V curves in (c) are averaged curves over areas indicated by black and red dashed rectangles, respectively, in (a) and (b). The red and black dotted curves are the dI/dV spectra numerically differentiated from the red and black I-V curves, respectively.

have reversed spin contrast between regions of even and odd layer thickness, like the islands and terraces in Fig. 2. With this model, one can explain the reversed contrast areas together with the dip region in topography by assuming the existence of Co islands below the Mn film, as sketched in Fig. 1(a). The numbers there correspond to those in Fig. 1(d), indicating different cases of Mn film grown on the Co surface. The difference in apparent height is not likely to result from the spin-dependent electronic contribution since this will give higher apparent height for parallel (or anti-parallel) configuration. This is not consistent with our data in Fig. 2, where the reversed contrast areas on islands and on the terrace have opposite spin contrast but are both lower than the surrounding atoms. Because the difference between the interlayer distance of Co and Mn is 16 pm (Co 174 pm and Mn 190 pm (Ref. 27)), the presence of a Co island along with a reduced thickness of the Mn film grown on top by one monolayer, as compared to the surrounding Mn film, will thus result in a region of 16 pm dip in topography. Combined with a layerwise spin component, this dip region will then have reversed spin contrast. Similarly, for Mn overgrowing a Co step edge, like between cases 1 and 2 in Fig. 1(a), there should also be a height difference of 16 pm in line profile across the step edge, together with the reversal of the spin contrast. This is consistent with the result in Fig. 1(d). The discrepancy between our measured value, i.e., 20 pm, and the value in Ref. 27 might come from the calibration of the Z piezo, since the interlayer distance of Mn is measured to be 201 pm, which is also larger than the value of 189 pm in Ref. 27. In Fig. 2, the lateral size of these dip areas is around several nanometers, quite similar to that of Co islands grown at room temperature, as shown in Fig. 1(b). The spin asymmetry in Fig. 2, defined by $|\sigma_p - \sigma_{ap}|/(\sigma_p + \sigma_{ap})$, where σ_p and σ_{ap} are the differential conductances in parallel and anti-parallel configurations, respectively, is about 14%, and the signal-to-noise ratio, defined by $|\sigma_p - \sigma_{ap}|$/width of the peak, is around 1.8. This further supports the layerwise spin component model of Mn/Co/Cu(001), and thus proves that such bulk Fe rings can be used as probe of SP-STM.

As for the issue of spatial resolution, since the sample studied here is based on a single crystal substrate, the surface is quite flat, such that a tiny protrusion at the ring's end will dominate the tunneling current. This means the spatial resolution will not be limited by the bulk ring. Actually, even atomic resolution has been achieved by a bulk W ring.[28] The spatial resolution defined by the transition width across a monoatomic step edge is measured to be less than one nanometer, similar to the result of Ref. 20. This is usually larger than the resolution obtained on a terrace due to the non-perpendicular tunneling across the edge.

In summary, using a bulk Fe ring as the scanning probe we have realized SP-STM at room temperature in ultrahigh vacuum on Mn/Co/Cu(001). It provides a simpler preparation procedure and better control over the probe's magnetizaton direction as compared to Fe-coated W ring probes. We found a layerwise antiferromagnetic spin structure of the Mn layer, which reflects overgrown monoatomic islands and step edges of the ferromagnetic Co layer underneath. With two probes the ring planes of which are perpendicular to each other, one can in principle resolve the spin polarization direction of the sample if the same area is scanned. For samples with flat surfaces and in-plane spin structure, the bulk Fe ring probe provides a convenient method to study their surface spin structure with SP-STM.

[1]M. Bode, Rep. Prog. Phys. **66**, 523 (2003).
[2]S. Heinze, M. Bode, A. Kubetzka, O. Pietzsch, X. Nie, S. Blügel, and R. Wiesendanger, Science **288**, 1805 (2000).
[3]R. Wiesendanger, D. Bürgler, G. Tarrach, T. Schaub, U. Hartmann, H. J. Güntherodt, I. V. Shvets, and J. M. D. Coey, Appl. Phys. A **53**, 349 (1991).
[4]R. Koltun, M. Herrmann, G. Güntherodt, and V. Brabers, Appl. Phys. A **73**, 49 (2001).
[5]S. Ceballos, G. Mariotto, S. Murphy, and I. Shvets, Surf. Sci. **523**, 131 (2003).
[6]M. Cavallini and F. Biscarini, Rev. Sci. Instrum. **71**, 4457 (2000).
[7]C. Albonetti, I. Bergenti, M. Cavallini, V. Dediu, M. Massi, J. F. Moulin, and F. Biscarini, Rev. Sci. Instrum. **73**, 4254 (2002).
[8]M. V. Rastei and J. P. Bucher, J. Phys.: Condens. Matter **18**, L619 (2006).
[9]P. J. Hsu, C. I. Lu, S. W. Chen, W. J. Hsueh, Y. H. Chu, C. H. Hsu, C. J. Butler, and M. T. Lin, Appl. Phys. Lett. **96**, 142515 (2010).
[10]I. V. Shvets, R. Wiesendanger, D. Bürgler, G. Tarrach, H. J. Güntherodt, and J. M. D. Coey, J. Appl. Phys. **71**, 5489 (1992).
[11]S. Murphy, J. Osing, and I. Shvets, Appl. Surf. Sci. **144–145**, 497 (1999).
[12]A. L. Bassi, C. S. Casari, D. Cattaneo, F. Donati, S. Foglio, M. Passoni, C. E. Bottani, P. Biagioni, A. Brambilla, M. Finazzi, F. Ciccacci, and L. Duo, Appl. Phys. Lett. **91**, 173120 (2007).
[13]N. Berdunov, S. Murphy, G. Mariotto, and I. V. Shvets, Phys. Rev. Lett. **93**, 057201 (2004).
[14]M. Bode, M. Getzlaff, and R. Wiesendanger, Phys. Rev. Lett. **81**, 4256 (1998).
[15]J. Prokop, A. Kukunin, and H. J. Elmers, Phys. Rev. Lett. **95**, 187202 (2005).
[16]A. Kubetzka, M. Bode, O. Pietzsch, and R. Wiesendanger, Phys. Rev. Lett. **88**, 057201 (2002).
[17]H. Yang, A. R. Smith, M. Prikhodko, and W. R. L. Lambrecht, Phys. Rev. Lett. **89**, 226101 (2002).

[18]W. Wulfhekel, H. Ding, and J. Kirschner, J. Magn. Magn. Mater. **242–245** (Part 1), 47 (2002).
[19]U. Schlickum, W. Wulfhekel, and J. Kirschner, Appl. Phys. Lett. **83**, 2016 (2003).
[20]C. B. Wu, P. J. Hsu, H. Y. Yen, and M. T. Lin, Appl. Phys. Lett. **91**, 202507 (2007).
[21]J. T. Kohlhepp, H. Wieldraaijer, and W. J. M. de Jonge, Appl. Phys. Lett. **89**, 032507 (2006).
[22]J. T. Kohlhepp and W. J. M. de Jonge, Phys. Rev. Lett. **96**, 237201 (2006).
[23]H. F. Ding, J. E. Pearson, D. Li, R. Cheng, F. Y. Fradin, and S. D. Bader, Rev. Sci. Instrum. **76**, 123703 (2005).
[24]S. Krause, L. Berbil-Bautista, G. Herzog, M. Bode, and R. Wiesendanger, Science **317**, 1537 (2007).
[25]U. Schlickum, N. Janke-Gilman, W. Wulfhekel, and J. Kirschner, Phys. Rev. Lett. **92**, 107203 (2004).
[26]D. Wortmann, S. Heinze, P. Kurz, G. Bihlmayer, and S. Blügel, Phys. Rev. Lett. **86**, 4132 (2001).
[27]J. T. Kohlhepp, J. Phys. D: Appl. Phys. **40**, 1300 (2007).
[28]P. J. Hsu and M. T. Lin, in *Microscopy: Science, Technology, Applications and Education*, edited by A. Méndez-Vilas and J. Díaz (FORMATEX, Badajoz, 2010), Vol. 3, p. 2001.
[29]P. J. Hsu, C. I. Lu, Y. H. Chu, B. Y. Wang, C. B. Wu, L. J. Chen, S. S. Wong, and M. T. Lin, Phys. Rev. B **85**, 174434 (2012).
[30]P. J. Hsu, "Resolving magnetic spin structures by spin-polarized scanning tunneling microscopy: Antiferromagnetic ultrathin Mn films and ferromagnetic Co nanoislands," Doctoral dissertation (National Taiwan University, 2010)